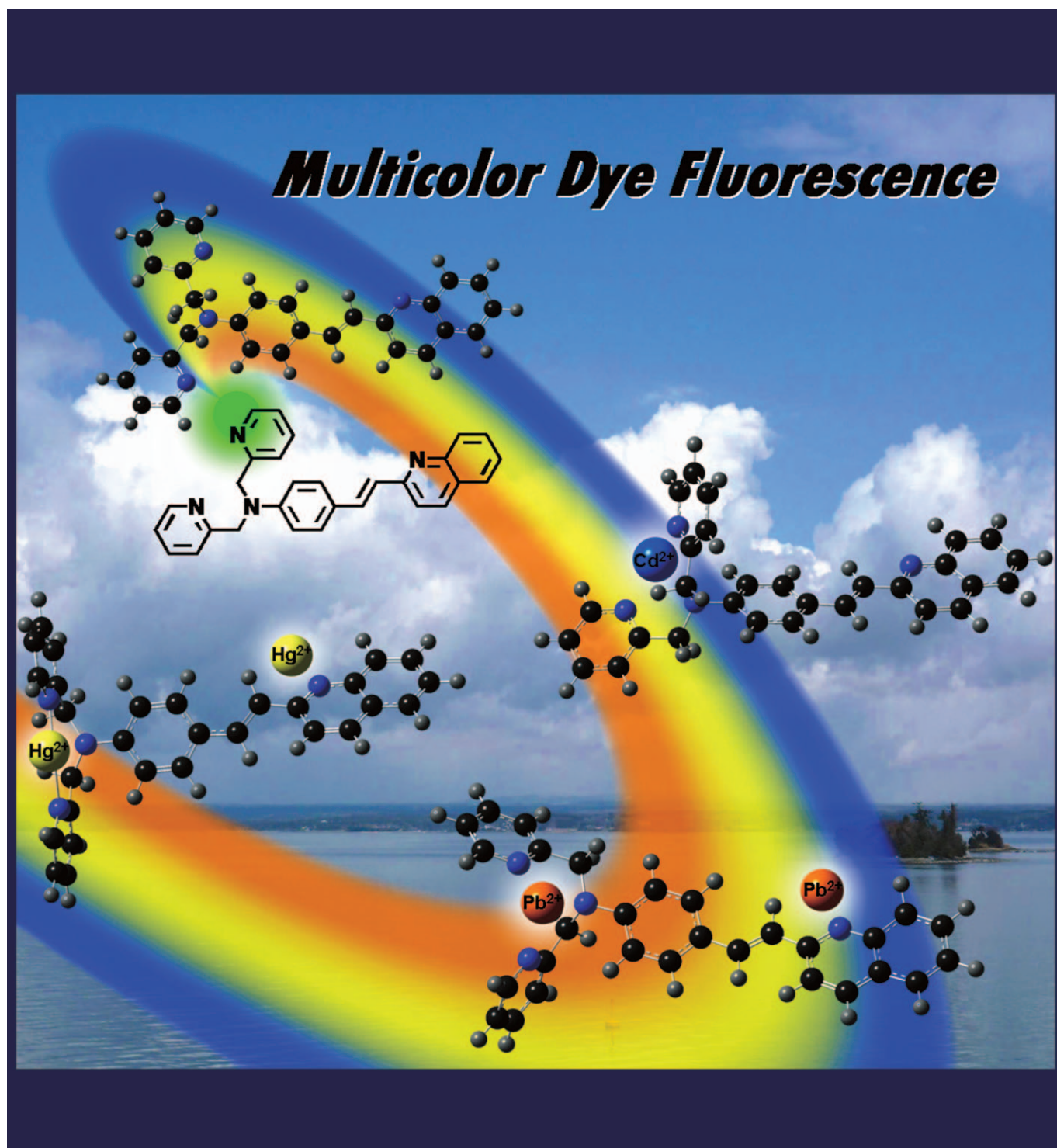


Multicolor Fluorescence of a Styrylquinoline Dye Tuned by Metal Cations

Yasuhiro Shiraishi,* Chizuru Ichimura, Shigehiro Sumiya, and Takayuki Hirai^[a]



Abstract: A styrylquinoline dye with a dipicolylamine (DPA) moiety (**1**) has been synthesized. The dye **1** in acetonitrile demonstrates multicolor fluorescence upon addition of different metal cations. Compound **1** shows a green fluorescence without cations. Coordination of **1** with Cd^{2+} shows a blue emission, while with Hg^{2+} and Pb^{2+} exhibits yellow and orange emissions, respectively. The different fluorescence spectra are due to the change in intramolecular charge transfer (ICT) properties of **1** upon coordination with

different cations. The DPA and quinoline moieties of **1** behave as the electron donor and acceptor units, respectively, and both units act as the coordination site for metal cations. Cd^{2+} coordinates with the DPA unit. This reduces the donor ability of the unit and decreases the energy level of HOMO. This results in an increase in HOMO–

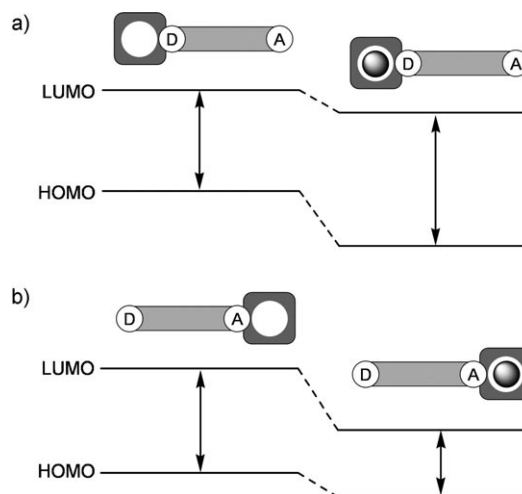
LUMO gap and blue shifts the emission. Hg^{2+} or Pb^{2+} coordinate with both DPA and quinoline units. The coordination with the quinoline unit decreases the energy level of LUMO. This results in a decrease in HOMO–LUMO gap and red shifts the emission. Addition of two different metal cations successfully creates intermediate colors; in particular, the addition of Cd^{2+} and Pb^{2+} at once creates a bright white fluorescence.

Keywords: charge transfer • dyes/pigments • fluorescence • transition metals • white emission

Introduction

Organic light-emitting dyes have attracted much attention in the optical electronics industry, because of their potential applications in displays and light sources.^[1] It is, however, known that a single dye molecule usually shows a single fluorescence. Creation of representative fluorescence colors, typically violet, indigo, blue, green, yellow, orange, and red,^[2] therefore requires the dyes to show respective fluorescence colors, and intermediate colors to be created by mixing these dyes.^[3] In particular, a white fluorescence color is very difficult to create; three kinds of dyes that show blue, green, and red fluorescence or two kinds of dyes that show blue and yellow fluorescence must be mixed in appropriate amounts.^[4] Recently, dyes that show multiple fluorescence colors in response to external stimuli have attracted much attention because these can create multiple fluorescence colors with a single molecule.^[5] Several external stimuli have been used for modulation of emission colors, such as excitation wavelength,^[6] temperature,^[7] pH,^[8] and solvent polarity.^[9]

Metal cations are often used as an external stimulus for modulation of fluorescence colors.^[10] The most popular molecular systems showing metal-induced fluorescence change are the intramolecular charge transfer (ICT) systems,^[11] which consist of an electron donor and acceptor units coupled through a π -conjugated spacer (Scheme 1). These ICT systems possess spatially separated frontier molecular orbitals.^[12] The interaction of the electron donor or acceptor moiety with metal cation, therefore, affects the energetic po-



Scheme 1. Schematic representation of the change in energy gap promoted by the coordination of metal cation.

sition of either HOMO or LUMO and elicits a change in fluorescence spectra. When the metal binding site is situated in the donor moiety (Scheme 1a), the coordination with a metal cation stabilizes the HOMO more strongly than LUMO, resulting in a blue shift of fluorescence spectra.^[13] In contrast, when the binding site is situated in the acceptor moiety (Scheme 1b), metal coordination stabilizes the LUMO more strongly than HOMO, resulting in a red shift of fluorescence spectra.^[14] Several ICT-based fluorescent dyes have been proposed; however, most of the dyes show only two^[14b,15] or three^[5b,16] fluorescence colors among the seven representative colors (violet, indigo, blue, green, yellow, orange, and red).

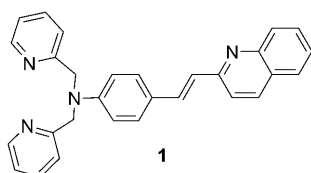
One of the possible ways to create multiple fluorescence colors is to construct metal binding sites on both the electron acceptor and donor moieties of the ICT systems. Coordination of metal cations with either the donor or acceptor moiety or with both moieties would promote change in the

[a] Dr. Y. Shiraishi, Dr. C. Ichimura, S. Sumiya, Prof. T. Hirai
Research Center for Solar Energy Chemistry and
Division of Chemical Engineering
Graduate School of Engineering Science
Osaka University, Toyonaka 560-8531 (Japan)
Fax: (+81) 6-6850-6271
E-mail: shiraish@cheng.es.osaka-u.ac.jp

Supporting information for this article is available on the WWW under <http://dx.doi.org/10.1002/chem.201101048>.

energetic positions of the HOMO and LUMO, and create multiple fluorescence colors. On the basis of this scenario, Bunz and co-workers synthesized a series of cruciform dyes (1,4-distyryl-2,5-bis(arylethynyl)benzene) possessing metal binding sites on both the donor and acceptor moieties.^[17] Addition of different metal cations to the solution containing these dyes create several emission colors, such as indigo–green–red,^[17a] blue–yellow–red,^[17b] indigo–blue–green,^[17c] blue–green–orange,^[17d] and indigo–green–orange.^[17e] Some other ICT-based dyes with two different metal binding sites have also been proposed.^[15b,18] All of these ICT systems,^[15b,17,18] however, show only three fluorescence colors among the seven representative colors.

Herein, we report an ICT-based dye that exhibits four types of fluorescence colors, namely, blue, green, yellow, and orange, upon coordination with different metal cations. The dye **1** consists of quinoline and dipicolylamine (DPA) moiety



ies that are connected through a π -conjugated vinyl spacer. The quinoline and DPA units behave as electron acceptor and donor units, respectively, and both units act as the metal binding site. The dye, when dissolved in MeCN, shows a green fluorescence. Addition of Cd^{2+} shows a blue emission, and addition of Hg^{2+} and Pb^{2+} exhibits yellow and orange emission, respectively. These emission properties are due to the different ICT properties of **1** in response to the coordination of the respective metal cations. Another notable feature of **1** is that the addition of two different metal cations at once successfully creates intermediate colors in correlation to the ratio of metal cations. In particular, a mixture of Cd^{2+} and Pb^{2+} creates a near-white fluorescence. To the best of our knowledge, this is the first report of dyes that creates a white fluorescence by a metal cation stimulus.

Results and Discussion

Fluorescence properties: The dye **1** was synthesized by the condensation of 2-methylquinoline with 4-(di-2-picolylamino)-benzaldehyde^[13a] in 47% yield (see Experimental Section). The purity of **1** was fully confirmed by ^1H and ^{13}C NMR spectroscopy, and FAB-MS analysis (Figures S1–S3 in the Supporting Information).

Figure 1a shows the fluorescence spectra of **1** (10 μM) measured in MeCN with and without each respective metal cation (10 equiv). Without a cation, **1** shows a green fluorescence at 508 nm ($\Phi_{\text{F}}=0.061$). Upon addition of Cd^{2+} , the spectrum blue shifts to 454 nm ($\Phi_{\text{F}}=0.033$). As shown in

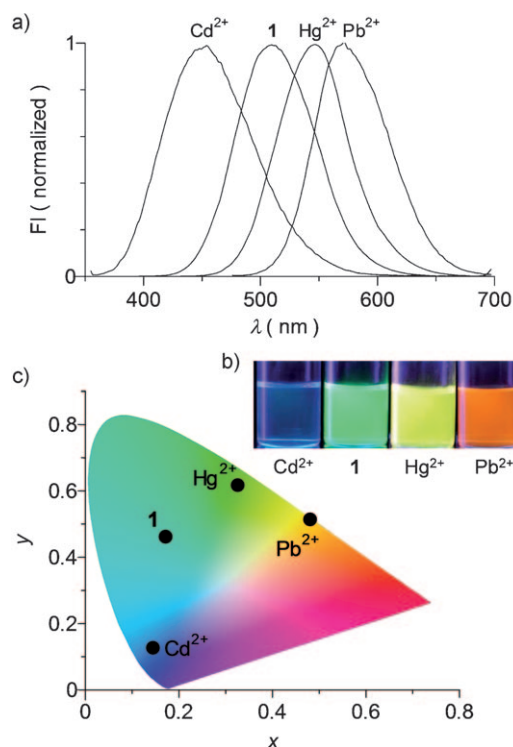


Figure 1. a) Fluorescence spectra of **1** (10 μM) measured in MeCN with 10 equivalents of each respective metal cation (as a ClO_4^- salt). The excitation wavelengths are 386 nm (free **1**), 350 nm (Cd^{2+}), 413 nm (Hg^{2+}), and 467 nm (Pb^{2+}), respectively. b) Fluorescence color of the respective solutions taken under irradiation with a handheld UV lamp (365 nm). c) Chromaticity of the fluorescence color of **1** obtained with and without metal cations in a 1931 CIE diagram.

Figure 1b, a bright blue emission is observed upon addition of Cd^{2+} . In contrast, addition of Hg^{2+} creates a red-shifted fluorescence at 546 nm with a yellow emission color ($\Phi_{\text{F}}=0.020$). Addition of Pb^{2+} shows a further red-shifted fluorescence at 571 nm with an orange emission color ($\Phi_{\text{F}}=0.010$). Figure 1c shows the CIE (International Commission on Illumination) chromaticity diagram^[19] for the fluorescence spectra. The free **1** shows a green fluorescence color with a chromaticity coordinate (0.17, 0.46), while the addition of respective cations shows a broad color range; Cd^{2+} (blue; 0.15, 0.13), Hg^{2+} (yellow; 0.33, 0.61), and Pb^{2+} (orange; 0.46, 0.52). These indicate that **1** creates four types of fluorescence colors among the seven representative colors upon addition of different metal cations. The fluorescence lifetimes of these emissions are similar to each other (0.6–1.2 ns, Figure S4, Supporting Information). It is also noted that, as shown in Figure S5 in the Supporting Information, addition of Zn^{2+} to the solution containing **1** shows a blue emission (441 nm; $\Phi_{\text{F}}=0.031$) similar to that of Cd^{2+} . Addition of Fe^{2+} , Fe^{3+} , or Cr^{3+} gives an orange emission (at 571 nm) similar to that of Pb^{2+} , although with decreased quantum yield ($\Phi_{\text{F}}<0.008$). Addition of other cations, such as Mn^{2+} , Ni^{2+} , Co^{2+} , and Cu^{2+} leads to almost no fluorescence.

Coordination properties: Fluorescence titration of **1** was carried out to clarify the coordination properties with metal cations. Figure 2a shows the result of fluorescence titration with Cd^{2+} . The Cd^{2+} addition leads to a decrease in the 508 nm fluorescence for free **1** and an increase in a blue-shifted fluorescence at 454 nm, with an isoemissive point at 461 nm. The spectral change almost terminates by the addition of one equivalent of Cd^{2+} . Figure 3a shows the result of absorption titration of **1** with Cd^{2+} . The absorption band at 386 nm associated with free **1** decreases with the addition of Cd^{2+} , with an isosbestic point at 350 nm. The spectral change is virtually finished with the addition of one equivalent of Cd^{2+} , which is consistent with the fluorescence titration data (Figure 2a). Nonlinear fitting of the absorption titration data by the Hyperquad program^[20] reveals that **1** coordinates with Cd^{2+} in a 1:1 stoichiometry with an association constant $\log K=6.5$ (Table 1). The dotted lines in the

Table 1. The apparent stability constants ($\log K$) of **1** with metal cations measured in MeCN at 298 K.^[a]

Reaction	Cd^{2+}	Hg^{2+}	Pb^{2+}
$\mathbf{1} + \text{M}^{2+} \rightarrow [\text{M}(\mathbf{1})]^{2+}$	6.5	7.0	5.1
$\mathbf{1} + 2\text{M}^{2+} \rightarrow [\text{M}_2(\mathbf{1})]^{4+}$		12.5	10.2

[a] Determined by Hyperquad program with the absorption titration data (Figure 3).

inset of Figure 2a show the mole fraction distribution of the species determined by the Hyss program^[21] with the association constant. The decrease in the 508 nm fluorescence agrees reasonably well with the formation of 1:1 **1**/ Cd^{2+} complex, suggesting that 1:1 coordination produces the blue-shifted fluorescence. The DPA ligand strongly coordinates with Cd^{2+} ,^[22] indicating that the coordination of DPA moiety of **1** with Cd^{2+} produces the 1:1 **1**/ Cd^{2+} complex.

Addition of Hg^{2+} or Pb^{2+} to **1** shows different fluorescence properties. In the case of Hg^{2+} (Figure 2b), addition of <1.5 equivalents of Hg^{2+} leads to a quenching of 508 nm fluorescence for the free **1**, but further Hg^{2+} addition creates a red-shifted fluorescence at 546 nm. This implies that two kinds of species are produced by the coordination of **1** with Hg^{2+} . Absorption titration data show a similar trend (Figure 3b). Addition of <1.5 equivalents of Hg^{2+} leads to a decrease in 386 nm absorption for the free **1** along with an increase in 356 nm band; however, further Hg^{2+} addition leads to a decrease in this band with an appearance of a new band at 402 nm. Nonlinear fitting analysis of the titration data indicates that 1:1 **1**/ Hg^{2+} ($\log K=7.0$) and 1:2 **1**/ Hg^{2+} complexes ($\log K=12.5$) are produced via a coordination of **1** with Hg^{2+} (Table 1). As shown in Figure 2b (inset), the fluorescence intensity decreases with the addition of approximately 1.5 equivalents of Hg^{2+} , which is in accordance with the 1:1 **1**/ Hg^{2+} complex formation. Further Hg^{2+} addition creates a red-shifted emission along with the 1:2 **1**/ Hg^{2+} complex formation. This suggests that the 1:2 **1**/ Hg^{2+} complex is the yellow emitting species.

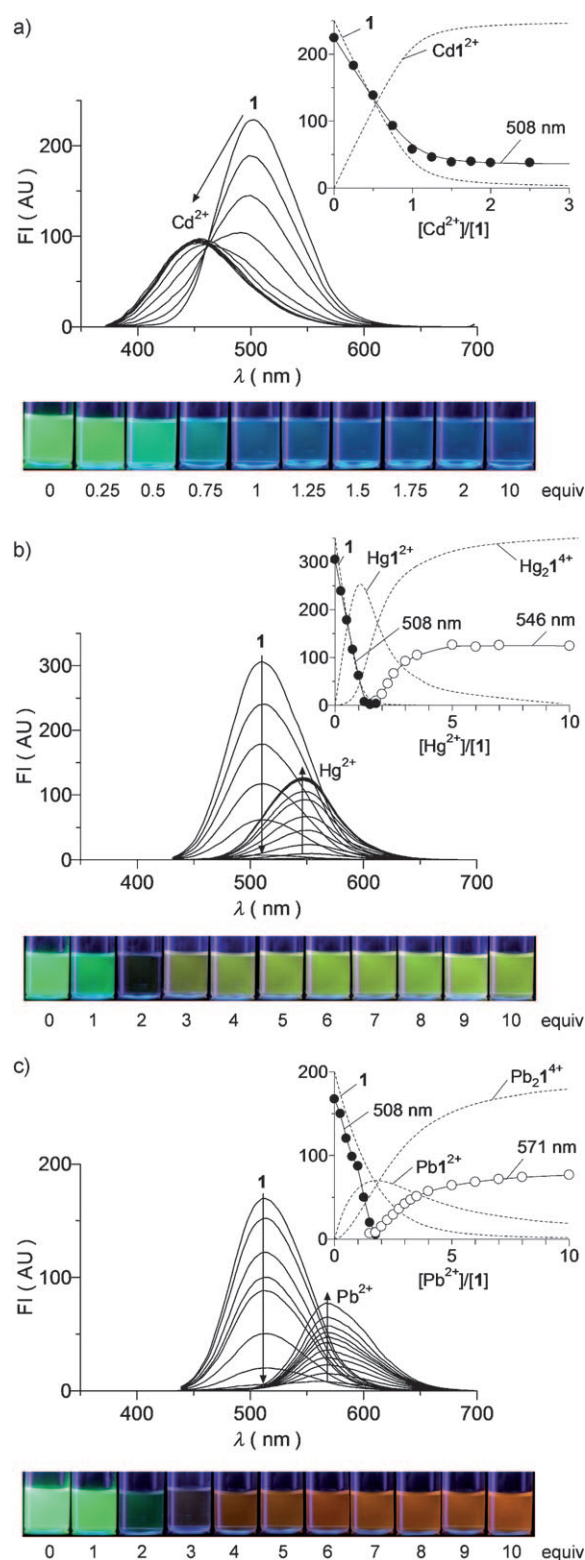


Figure 2. Fluorescence spectra of **1** (10 μM) measured in MeCN with different amount of a) Cd^{2+} ($\lambda_{\text{ex}}=350$ nm), b) Hg^{2+} ($\lambda_{\text{ex}}=413$ nm), and c) Pb^{2+} ($\lambda_{\text{ex}}=427$ nm). Inset: Change in fluorescence intensity, in which the dotted lines are the mole fraction distribution of species determined by the stability constants (Table 1). The photographs of the solutions were taken under irradiation with a handheld UV lamp (365 nm).

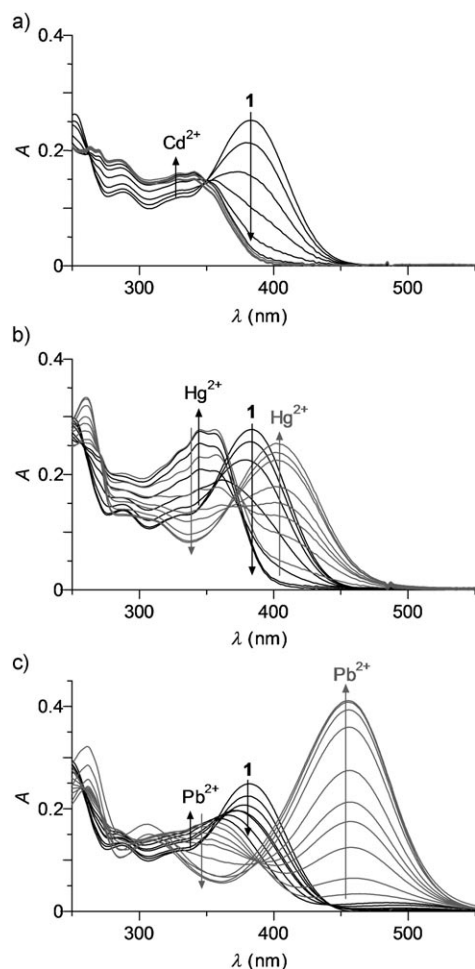


Figure 3. Absorption spectra of **1** (10 μM) measured in MeCN with different amount of a) Cd^{2+} , b) Hg^{2+} , and c) Pb^{2+} . The gray lines are the spectra obtained with 1.5–10.0 equivalents of metal cations.

Addition of Pb^{2+} shows spectral behaviors similar to that of Hg^{2+} . Nonlinear fitting of the absorption titration data (Figure 3c) also confirms the formation of 1:1 **1**/ Pb^{2+} ($\log K=5.1$) and 1:2 **1**/ Pb^{2+} ($\log K=10.2$) complexes (Table 1). As shown in Figure 2c (inset), addition of <1.5 equivalents of Pb^{2+} leads to a quenching of 508 nm fluorescence for the free **1** along with the 1:1 **1**/ Pb^{2+} complex formation. Further Pb^{2+} addition creates a red-shifted emission at 571 nm, which is in accordance with the 1:2 **1**/ Pb^{2+} complex formation. These suggest that the 1:2 **1**/ Pb^{2+} complex is the orange emitting species. As shown in Figure 3b and c, addition of <1.5 equivalents of Hg^{2+} or Pb^{2+} promotes a blue-shift of the absorption spectra, as is the case for Cd^{2+} . This indicates that the DPA unit of **1** firstly coordinates with Hg^{2+} or Pb^{2+} , producing nonemissive 1:1 **1**/ Hg^{2+} and **1**/ Pb^{2+} complexes. As quinoline nitrogen atoms can also coordinate with heavy metal cations such as Hg^{2+} and Pb^{2+} ,^[23] further addition of these ions leads to a coordination with the quinoline nitrogen, resulting in the formation of emissive 1:2 **1**/ Hg^{2+} and **1**/ Pb^{2+} complexes.

Change in electronic properties by metal cation binding: To clarify the change in electronic properties of **1** upon coordination with different metal cations, ab initio calculations were performed within the Gaussian 03 program by using the time-dependent density functional theory (TDDFT).^[24] As shown in Table S1 (in the Supporting Information), the singlet electronic transitions of free **1** and its metal complexes are mainly contributed by HOMO→LUMO or HOMO→LUMO+1 transition ($S_0 \rightarrow S_1$ or $S_0 \rightarrow S_2$), and the calculated transition energies are close to the observed absorption maxima of the spectra (Figure 3). This suggests that the calculated results represent the electronic properties of the compounds precisely.

Fluorescent dyes exhibiting ratiometric response to metal cations have spatially separated frontier molecular orbitals. The change in fluorescence properties upon metal cation coordination are therefore explained by the HOMO–LUMO gap and their electronic distributions.^[12] Figure 4 summarizes the energy levels of HOMO and LUMO for respective molecules and their electronic distributions. In the case of free **1** (Figure 4a), π electrons on the HOMO are mainly located on the aminostyrene moiety, whereas those on the LUMO are mainly located on the quinoline moiety. This indicates that the ICT from the donor (DPA) to the acceptor (quinoline) indeed occurs in the compound **1**.

Upon coordination of Cd^{2+} with the DPA unit (Figure 4b), the energy levels of both HOMO and LUMO decrease relative to those of free **1**. The HOMO level decreases more significantly, indicating that the HOMO is more stabilized than LUMO. Upon coordination of Cd^{2+} , π electrons on HOMO are distributed on the styrylquinoline moiety, in which the electrons are not located on the aniline nitrogen. This suggests that coordination of Cd^{2+} with the DPA moiety indeed decreases the electron-donating ability of the nitrogen atom of DPA moiety, as schematically shown in Scheme 1a.^[13a] The HOMO–LUMO gap therefore becomes larger relative to free **1**. This thus results in a blue shift of fluorescence spectra upon coordination with Cd^{2+} .

Coordination of Hg^{2+} or Pb^{2+} with the DPA moiety of **1** shows different electronic properties. As shown in Figure 4c and d, the HOMO and LUMO levels of the 1:1 **1**/ Hg^{2+} and **1**/ Pb^{2+} complexes are similar to those of 1:1 **1**/ Cd^{2+} complex (Figure 4b). The π electrons on LUMO of the 1:1 **1**/ Cd^{2+} complex are distributed on the styrylquinoline moiety, but those of the 1:1 **1**/ Hg^{2+} and **1**/ Pb^{2+} complexes are localized on the pyridine moieties. As shown in Table S2 (in the Supporting Information), π electron distribution on the styrylquinoline moiety exists at higher energy levels than LUMO+1. This is probably because the pyridine nitrogen atoms strongly coordinate with Hg^{2+} and Pb^{2+} , and the π electrons on the pyridine moieties are stabilized strongly.^[23] These results indicate that photoexcitation of these 1:1 **1**/ Hg^{2+} and **1**/ Pb^{2+} complexes promotes an electronic population of pyridine moieties by means of an electron-transfer process^[25] and, hence, shows almost no fluorescence.

Coordination of Hg^{2+} or Pb^{2+} with a quinoline moiety (formation of the 1:2 **1**/ Hg^{2+} and **1**/ Pb^{2+} complexes) alters

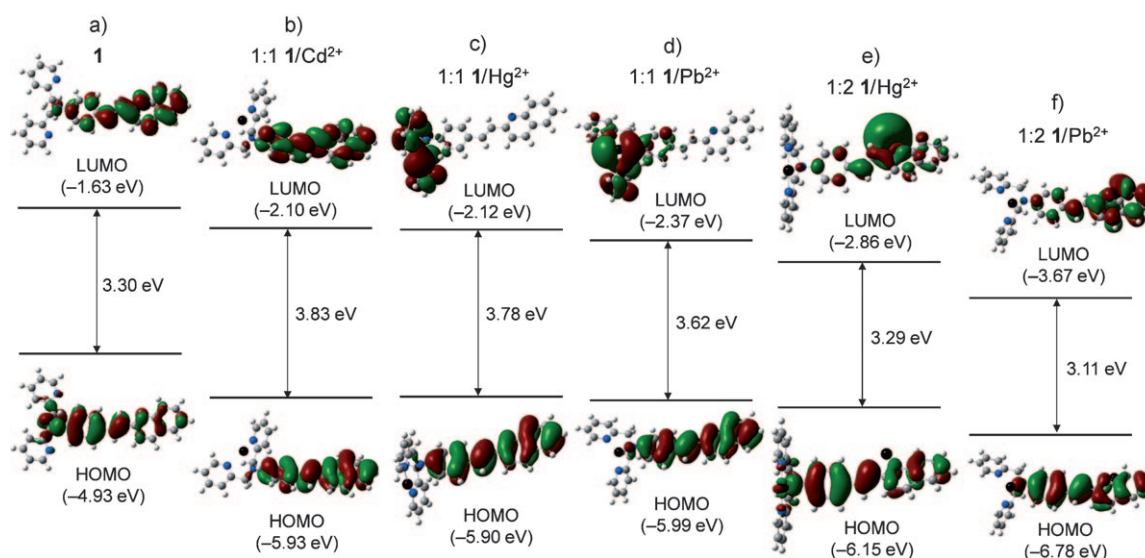


Figure 4. The HOMO–LUMO energy gaps for respective compounds and interfacial plots of the orbitals. a) free **1**, b) 1:1 **1**/Cd²⁺ complex, c) 1:1 **1**/Hg²⁺ complex, d) 1:1 **1**/Pb²⁺ complex, e) 1:2 **1**/Hg²⁺ complex, and f) 1:2 **1**/Pb²⁺ complex. Gray, blue, and black atoms of the molecular frameworks indicate the C, N, and metal atoms. Green and deep red parts on the interfacial plots refer to the different phase of the molecular wave functions, for which the isovalue is 0.02 a.u.

the electronic properties. As shown in Figure 4e and f, π electron distributions on HOMO of the 1:2 **1**/Hg²⁺ and **1**/Pb²⁺ complexes are similar to those of the corresponding 1:1 complexes. However, π electrons on LUMO of the 1:2 complexes are distributed on the quinoline moiety, whereas the 1:1 complexes have a π electron distribution on the pyridine moieties. This is probably because the coordination of the quinoline nitrogen with Hg²⁺ or Pb²⁺ stabilizes π electrons on the quinoline moiety. The 1:2 complexes have lower HOMO and LUMO energy levels than those of free **1**. The decrease in the LUMO level is more significant than that of the HOMO, indicating that the LUMO is more stabilized. The π electrons on the LUMO of the 1:2 **1**/Hg²⁺ and **1**/Pb²⁺ complexes are localized on the quinoline moiety, whereas the free **1** and 1:1 **1**/Cd²⁺ complex have a π electron distribution on the aminostyrene moieties. This suggests that the 1:2 **1**/Hg²⁺ and **1**/Pb²⁺ complexes strongly promote the ICT from the donor DPA to the acceptor quinoline moieties, through the stabilization of LUMO by the coordination of Hg²⁺ or Pb²⁺ with the quinoline nitrogen, as schematically shown in Scheme 1b. This therefore leads to a decrease in the HOMO–LUMO gap and results in a red-shift of the fluorescence spectra.^[14a,26]

Effect of mixing two metal cations: The effect of mixing two metal cations on the fluorescence spectra of **1** was studied to clarify whether the intermediate colors can be created according to the ratio of mixed metal cations. Figure 5 shows the fluorescence spectra of **1** (20 μ M) measured with two metal cations (Cd²⁺/Hg²⁺, Hg²⁺/Pb²⁺, and Cd²⁺/Pb²⁺) as a function of the metal cation ratio, for which the total metal cation concentrations are set at 200 μ M. As shown in Figure 5a, Cd²⁺/Hg²⁺ mixtures show two fluorescence bands at 454 and 546 nm, assigned to the 1:1 **1**/Cd²⁺ and 1:2 **1**/Hg²⁺

complexes, and the intensity of respective bands changes with the Cd²⁺/Hg²⁺ ratio. At high Cd²⁺ concentration, the 1:1 **1**/Cd²⁺ complex exists and shows 454 nm fluorescence. Addition of Hg²⁺ leads to a formation of non-emissive 1:1 **1**/Hg²⁺ complex, through the replacement of Cd²⁺ with Hg²⁺, due to the higher stability constant between the DPA unit and Hg²⁺ than Cd²⁺ (Table 1) and results in the quenching of 454 nm fluorescence. Further Hg²⁺ addition promotes coordination of quinoline nitrogen with Hg²⁺ (formation of 1:2 **1**/Hg²⁺ complex) and shows 546 nm fluorescence. As shown in Figure 6 (white circle), the chromaticity coordinates of Cd²⁺/Hg²⁺ mixtures lie in a near straight line connecting those for pure Cd²⁺ and Hg²⁺ solutions. This indicates that, in the mixtures, the replacement and sequential coordination of metal cations successfully creates intermediate colors.^[19]

Figure 5b shows the fluorescence spectra of Hg²⁺/Pb²⁺ mixtures. The change in Hg²⁺/Pb²⁺ ratio leads to a continuous shift of the spectra at between 546 and 571 nm, which are assigned to the 1:2 **1**/Hg²⁺ and **1**/Pb²⁺ complexes, respectively. At high Pb²⁺ concentration, 1:2 **1**/Pb²⁺ complex exists and shows fluorescence at 571 nm. The increase in Hg²⁺ concentration probably leads to a formation of binuclear 1:1:1 **1**/Hg²⁺/Pb²⁺ complex, in which the DPA and quinoline units coordinate with Hg²⁺ and Pb²⁺, respectively, due to the higher stability constant between the DPA unit and Hg²⁺ than Pb²⁺ (Table 1). This probably results in continuous blue shift of the spectra. Further Hg²⁺ increase leads to a replacement of Pb²⁺ coordinated by quinoline nitrogen with Hg²⁺ (formation of 1:2 **1**/Hg²⁺ complex). This results in further blue shift of the spectra. As shown in Figure 6 (square), the chromaticity coordinates of Hg²⁺/Pb²⁺ mixture lies in a straight line connecting those for pure Hg²⁺ and Pb²⁺ solutions. This indicates that continuous blue

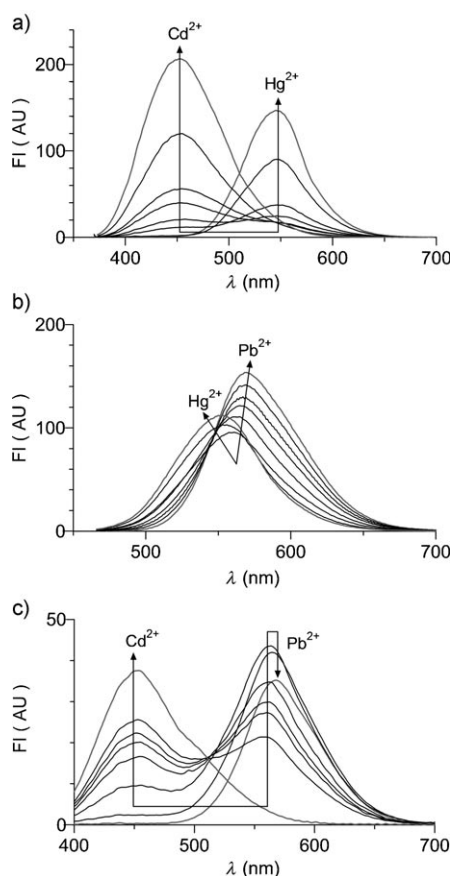


Figure 5. Fluorescence spectra of **1** (20 μM) measured in MeCN in the presence of a) Cd²⁺/Hg²⁺ mixture (Cd²⁺ + Hg²⁺ = 10 equiv, λ_{ex} = 365 nm), b) Hg²⁺/Pb²⁺ (Hg²⁺ + Pb²⁺ = 10 equiv, λ_{ex} = 454 nm), and c) Cd²⁺/Pb²⁺ (Cd²⁺ + Pb²⁺ = 10 equiv, λ_{ex} = 390 nm), as a function of the ratio of metal cations. The metal cation ratios are: a) Cd²⁺/Hg²⁺ = 10:0, 9.5:0.5, 9.2:0.8, 9:1, 8.9:1.1, 8.7:1.3, 8:2, 0:10; b) Hg²⁺/Pb²⁺ = 10:0, 2:8, 1:9, 0.8:9.2, 0.5:9.5, 0.3:9.7, 0.1:9.9, 0:10; c) Cd²⁺/Pb²⁺ = 10:0, 8.5:1.5, 8:2, 7.5:2.5, 7:3, 6:4, 2:8, 0:10. The gray lines are the spectra obtained ratios with 10:0 and 0:10. The absorption spectra and photographs for respective solutions are summarized in Figure S6 and S7, respectively (Supporting Information).

shift of the spectra by the sequential replacement of metal cations allows successful creation of intermediate colors.

Figure 5c shows the fluorescence spectra of Cd²⁺/Pb²⁺ mixture. At high Cd²⁺ concentration, 1:1 **1**/Cd²⁺ complex exists and shows 454 nm fluorescence. Addition of Pb²⁺ leads to a decrease in the 454 nm fluorescence along with an appearance of 563 nm fluorescence, with an isoemissive point at 512 nm. The ratiometric spectral change is probably due to the coordination of quinoline nitrogen with Pb²⁺, leading to a formation of binuclear 1:1:1 **1**/Cd²⁺/Pb²⁺ complex, in which the DPA and quinoline units coordinate with Cd²⁺ and Pb²⁺, respectively. Further increase in Pb²⁺ concentration leads to a decrease in 563 nm fluorescence with a red shift of the spectrum (571 nm). This is because the replacement of Cd²⁺ coordinated by DPA unit with Pb²⁺ leads to a formation 1:2 **1**/Pb²⁺ complex. As shown in Figure 6 (triangle), the chromaticity coordinates of Cd²⁺/Pb²⁺ mixture draws a gentle curve connecting those for

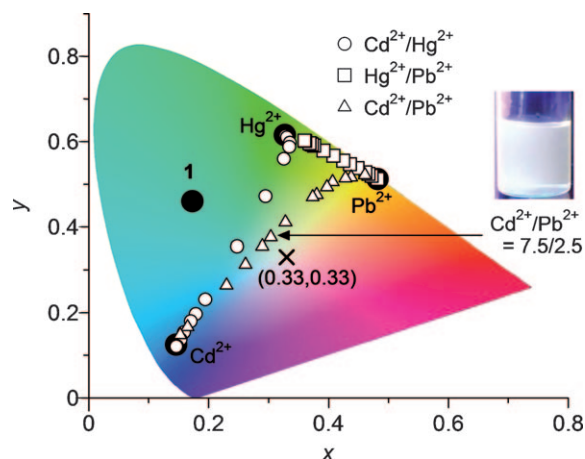


Figure 6. Chromaticity coordinates for fluorescence spectra of **1** (20 μM) measured with and without metal cations in a 1931 CIE diagram. ●: with pure metal cations, ○: Cd²⁺/Hg²⁺ mixtures, □: Hg²⁺/Pb²⁺ mixtures, △: Cd²⁺/Pb²⁺ mixtures. The total concentrations of cations in solutions are set at 200 μM. × denotes the ideal coordinate for white color fluorescence (0.33, 0.33). The photographs for respective solutions are summarized in Figure S7 (Supporting Information).

pure Cd²⁺ and Pb²⁺ solutions because of the formation of binuclear 1:1:1 **1**/Cd²⁺/Pb²⁺ complex. Nevertheless, the data indicate that the mixing of these metal cations successfully creates intermediate colors.

The above findings indicate that the mixing two metal cations with **1** enables creation of various intermediate fluorescence colors. Another notable feature of **1** is that a near white fluorescence color can be created. As indicated by the arrow in Figure 6 (triangle), the chromaticity coordinate of the mixture consisting of Cd²⁺ (7.5 equiv) and Pb²⁺ (2.5 equiv) is (0.31, 0.37), which is close to the standard white light illuminate (0.33, 0.33)^[4] indicated by a cross. As shown by the inset photograph, a bright white fluorescence (Φ_F = 0.014) is observed. Generally, a white fluorescence has to be created by mixing three kinds of dyes that show blue, green, and red fluorescence, or two kinds of dyes that show blue and yellow fluorescence.^[4] To the best of our knowledge, this is the first report of a dye that shows a white fluorescence induced by metal cations.

Conclusion

We clarified that a styrylquinoline dye containing a DPA moiety (**1**) shows multiple fluorescence colors upon coordination with different metal cations. The dye **1** has a green fluorescence, and shows different fluorescence colors in the presence of Cd²⁺ (blue), Hg²⁺ (yellow), and Pb²⁺ (orange). These color changes are explained by the ICT process within the molecule. The dye **1** possesses DPA and quinoline units that act as electron donor and acceptor, respectively, and both units behave as coordination sites for metal cations. The energy levels of HOMO and LUMO orbitals of **1** are critically changed by the coordination of different metal

cations and results in blue or red shift of the fluorescence spectra. Another notable feature of the dye is that the addition of two metal cations at once successfully creates intermediate colors according to the ratio of metal cations. In particular, the addition of the mixture of Cd^{2+} and Pb^{2+} with an appropriate ratio creates a near-white fluorescence. The basic molecular design used here based on the ICT molecules possessing metal-binding sites on both the electron donor and acceptor moieties may become a powerful tool for creation of multicolor fluorescence by metal cation inputs.

Experimental Section

Compound 1: 4-(Di-2-picolylamino)benzaldehyde^[13a] (0.39 g, 1.29 mmol), 2-methylquinoline (0.18 g, 1.29 mmol), and piperidine (100 μL) were dissolved in toluene (1 mL) and stirred at 110 °C for 16 h under dry nitrogen. Aqueous NaOH (0.1 M, 70 mL) solution was added to the resulting solution, and solution was extracted with CH_2Cl_2 (3×20 mL). The combined organic layer was dried over Na_2SO_4 , and concentrated by evaporation. The obtained solid was recrystallized from EtOH, affording **1** as an orange powder (0.26 g, yield 47%). ^1H NMR (270 MHz, CD_3Cl , TMS): $\delta = 4.87$ (s, 4H; CH_2), 6.74 (d, $J = 8.90$ Hz, 2H), 7.14–7.28 (m, 5H), 7.41–7.75 (m, 9H), 8.04 (t, $J = 8.49$ Hz, 2H), 8.61 ppm (d, $J = 4.29$ Hz, 2H); ^{13}C NMR (67.8 MHz, CDCl_3 , TMS): $\delta = 158.11$, 156.49, 149.56, 148.48, 148.06, 136.65, 135.80, 134.18, 130.57, 129.34, 128.75, 128.53, 127.21, 126.86, 125.60, 125.46, 124.88, 121.97, 120.61, 118.82, 112.47, 111.87, 57.17 ppm; FAB-MS: m/z calcd for $\text{C}_{29}\text{H}_{24}\text{N}_4$: 428.20; found: 429.22 $[\text{M}+\text{H}]^+$. HRMS (FAB+): m/z calcd for $\text{C}_{29}\text{H}_{23}\text{N}_4$: 429.2079; found: 429.2061 $[\text{M}+\text{H}]^+$. ^1H , ^{13}C NMR and FAB-MS charts are shown in Figures S1–S3 (Supporting Information).

Analysis: Fluorescence spectra were measured on a Hitachi F-4500 fluorescence spectrophotometer.^[27] Absorption spectra were measured on an UV-visible photodiode-array spectrophotometer (Shimadzu; Multispec-1500). The measurements were carried out at (298 ± 1) K using a 10 mm path length quartz cell. The spectra in the presence of metal cations were measured after stirring the solution for 1 min. Perchlorate salts were used as a metal source, and all measurements were carried out in an aerated condition. Fluorescence quantum yield (Φ_F) was determined by comparison of the integrated corrected emission spectrum of standard quinine, which was excited at 366 nm in H_2SO_4 (0.5 M, $\Phi_F = 0.55$).^[28] ^1H and ^{13}C NMR spectra were obtained by a JEOL JNM-GSX270 Excalibur. FAB-MS spectra were obtained by a JEOL JMS-700 Mass Spectrometer. The program HYPERQUAD was used for determination of stability constants for complexes.^[29] The mole fraction distribution of the species were obtained using the Hyss program.^[21]

Computational methods: Ab initio calculations were performed with the Gaussian 03 program.^[24] Geometry optimization was carried out with the density functional theory (DFT) using the B3LYP function. The metal-free compound was calculated using the 6-31G* basis set. Cd^{2+} complexes were calculated using the 6-31G* basis set for all atoms except for Cd^{2+} , for which the LANL2DZ basis set with effective core potential was used. The Hg^{2+} complex was calculated by using the 6-31G* basis set for all atoms except for Hg^{2+} , for which the Stuttgart relativistic small-core basis set with effective core potential was used. The Pb^{2+} complex was calculated using the 6-31G* basis set for all atoms except for Pb^{2+} , for which SDD basis set with effective core potential was used. The electronic excitation energies and oscillator strength were calculated with the time-dependent density functional theory (TDDFT).

Acknowledgements

This work was partly supported by the Grant-in-Aid for Scientific Research (No. 23656503) from the Ministry of Education, Culture, Sports, Science and Technology, Japan (MEXT). C.I. thanks the Global COE Program "Global Education and Research Center for Bio-Environmental Chemistry" of Osaka University.

- [1] a) C. W. Tang, S. A. VanSlyke, *Appl. Phys. Lett.* **1987**, *51*, 913–915; b) M. A. Baldo, M. E. Thompson, S. R. Forrest, *Nature* **2000**, *403*, 750–753.
- [2] T. J. White, M. E. McConney, T. J. Bunning, *J. Mater. Chem.* **2010**, *20*, 9832–9847.
- [3] a) T. R. Hebner, J. C. Sturm, *Appl. Phys. Lett.* **1998**, *73*, 1775–1777; b) C. W. Ko, Y. T. Tao, *Appl. Phys. Lett.* **2001**, *79*, 4234–4236; c) K. O. Cheon, J. Shinar, *Appl. Phys. Lett.* **2002**, *81*, 1738–1740; d) M. Mazzeo, D. Pisignano, F. D. Sala, J. Thompson, R. I. R. Blyth, G. Gigli, R. Cingolani, G. Sotgiu, G. Barbarella, *Appl. Phys. Lett.* **2003**, *82*, 334–336; e) D. Qin, Y. Tao, *Appl. Phys. Lett.* **2005**, *86*, 113507/1–113507/3.
- [4] a) S. Park, J. E. Kwon, S. H. Kim, J. Seo, K. Chung, S.-Y. Park, D.-J. Jang, B. M. Medina, J. Gierschner, S. Y. Park, *J. Am. Chem. Soc.* **2009**, *131*, 14043–14049; b) P. Coppo, M. Duati, V. N. Kozhevnikov, J. W. Hofstraat, L. D. Cola, *Angew. Chem.* **2005**, *117*, 1840–1844; *Angew. Chem. Int. Ed.* **2005**, *44*, 1806–1810; c) R. Abbel, C. Grenier, M. J. Pouderoijen, J. W. Stouwdam, P. E. L. G. Leclère, R. P. Sijbesma, E. W. Meijer, A. P. H. J. Schenning, *J. Am. Chem. Soc.* **2009**, *131*, 833–843; d) J. Luo, X. Li, Q. Hou, J. Peng, W. Yang, Y. Cao, *Adv. Mater.* **2007**, *19*, 1113–1117; e) A. Ajayaghosh, V. K. Praveen, S. Srinivasan, R. Varghese, *Adv. Mater.* **2007**, *19*, 411–415; f) J. H. Kim, P. Herguth, M.-S. Kang, A. K.-Y. Jen, Y.-H. Tseng, C.-F. Shu, *Appl. Phys. Lett.* **2004**, *85*, 1116–1118.
- [5] a) G. He, D. Guo, C. He, X. Zhang, X. Zhao, C. Duan, *Angew. Chem.* **2009**, *121*, 6248–6251; *Angew. Chem. Int. Ed.* **2009**, *48*, 6132–6135; b) H. S. Joshi, R. Jamshidi, Y. Tor, *Angew. Chem.* **1999**, *111*, 2887–2891; *Angew. Chem. Int. Ed.* **1999**, *38*, 2721–2725.
- [6] Y. Yang, M. Lowry, C. M. Schowalter, S. O. Fakayode, J. O. Escobedo, X. Xu, H. Zhang, T. J. Jensen, F. R. Fronczek, I. M. Warner, R. M. Strongin, *J. Am. Chem. Soc.* **2006**, *128*, 14081–14092.
- [7] a) C. Li, Y. Zhang, J. Hu, J. Cheng, S. Liu, *Angew. Chem.* **2010**, *122*, 5246–5250; *Angew. Chem. Int. Ed.* **2010**, *49*, 5120–5124; b) T. Barilero, T. L. Saux, C. Gosse, L. Jullien, *Anal. Chem.* **2009**, *81*, 7988–8000; c) C.-Y. Chen, C.-T. Chen, *Chem. Commun.* **2011**, *47*, 994–996.
- [8] a) Y. Shiraishi, Y. Tokitoh, G. Nishimura, T. Hirai, *Org. Lett.* **2005**, *7*, 2611–2614; b) T. Bura, P. Retailleau, G. Ulrich, R. Ziessel, *J. Org. Chem.* **2011**, *76*, 1109–1117; c) L. Albertazzi, B. Storti, L. Marchetti, F. Beltram, *J. Am. Chem. Soc.* **2010**, *132*, 18158–18167; d) Y.-L. Chiu, S.-A. Chen, J.-H. Chen, K.-J. Chen, H.-L. Chen, H.-W. Sung, *ACS Nano* **2010**, *4*, 7467–7474.
- [9] a) S.-L. Wang, G.-Y. Gao, T.-I. Ho, L.-Y. Yang, *Chem. Phys. Lett.* **2005**, *415*, 217–222; b) S.-L. Wang, T.-C. Lee, T.-I. Ho, *J. Photochem. Photobiol. A* **2002**, *151*, 21–26.
- [10] *Fluorescent Chemosensors for Ion and Molecular Recognition* (Ed.: A. Czarnik), American Chemical Society, Washington DC, **1993**.
- [11] a) B. Valeur, I. Leray, *Coord. Chem. Rev.* **2000**, *205*, 3–40; b) M. Glasbeek, H. Zhang, *Chem. Rev.* **2004**, *104*, 1929–1954.
- [12] A. J. Zuccherro, P. L. Mcgrier, U. H. F. Bunz, *Acc. Chem. Res.* **2010**, *43*, 397–408.
- [13] X. Peng, J. Du, J. Fan, J. Wang, Y. Wu, J. Zhao, S. Sun, T. Xu, *J. Am. Chem. Soc.* **2007**, *129*, 1500–1501.
- [14] a) L. Zhang, L. Zhu, *J. Org. Chem.* **2008**, *73*, 8321–8330; b) H.-G. Löhr, F. Vögtle, *Acc. Chem. Res.* **1985**, *18*, 65–72; c) J. V. Mello, N. S. Finney, *Angew. Chem.* **2001**, *113*, 1584–1586; *Angew. Chem. Int. Ed.* **2001**, *40*, 1536–1538.
- [15] a) X. Zhang, Y. Shiraishi, T. Hirai, *Org. Lett.* **2007**, *9*, 5039–5042; b) Y. Q. Li, J. L. Bricks, U. Resch-Genger, M. Spieles, W. Rettig, *J. Phys. Chem. A* **2006**, *110*, 10972–10984; c) S. A. Ahmed, M. Tanaka,

- H. Ando, K. Tawa, K. Kimura, *Tetrahedron* **2004**, *60*, 6029–6036; d) B. Nisar Ahamed, I. Ravikumar, P. Ghosh, *New J. Chem.* **2009**, *33*, 1825–1828.
- [16] a) T. Ogawa, J. Yuasa, T. Kawai, *Angew. Chem.* **2010**, *122*, 5236–5240; *Angew. Chem. Int. Ed.* **2010**, *49*, 5110–5114; b) X. Guo, Y. Zhou, D. Zhang, B. Yin, Z. Liu, C. Liu, Z. Lu, Y. Huang, D. Zhu, *J. Org. Chem.* **2004**, *69*, 8924–8931.
- [17] a) J. N. Wilson, U. H. F. Bunz, *J. Am. Chem. Soc.* **2005**, *127*, 4124–4125; b) M. Hauck, J. Schönhaber, A. J. Zuccherro, K. I. Hardcastle, T. J. J. Müller, U. H. F. Bunz, *J. Org. Chem.* **2007**, *72*, 6714–6725; c) J. Tolosa, A. J. Zuccherro, U. H. F. Bunz, *J. Am. Chem. Soc.* **2008**, *130*, 6498–6506; d) S. M. Brombosz, A. J. Zuccherro, R. L. Phillips, D. Vazquez, A. Wilson, U. H. F. Bunz, *Org. Lett.* **2007**, *9*, 4519–4522; e) J. Tolosa, K. M. Solntsev, L. M. Tolbert, U. H. F. Bunz, *J. Org. Chem.* **2010**, *75*, 523–534.
- [18] C. Lu, Z. Xu, J. Cui, R. Zhang, X. Qian, *J. Org. Chem.* **2007**, *72*, 3554–3557.
- [19] a) CIE (1932), *Commission Internationale de L'Eclairage Proceedings*, Cambridge University Press, Cambridge, **1931**; b) T. Smith, J. Guild, *Trans. Opt. Soc.* **1931**, *33*, 73–134.
- [20] A. Sabatini, A. Vacca, P. Gans, *Coord. Chem. Rev.* **1992**, *120*, 389–405.
- [21] Hyperquad Simulation and Speciation (HySS). © 2006 Protonic Software. P Gans, Protonic Software, 2 Templegate Avenue, Leeds LS15 0HD, England: L. Alderighi, P. Gans, A. Ienco, D. Peters, A. Sabatini, A. Vacca, *Coord. Chem. Rev.* **1999**, *184*, 311–318.
- [22] a) E. M. Nolan, S. J. Lippard, *Inorg. Chem.* **2004**, *43*, 8310–8317; b) E. M. Nolan, S. C. Burdette, J. H. Harvey, S. A. Hilderbrand, S. J. Lippard, *Inorg. Chem.* **2004**, *43*, 2624–2635.
- [23] A. E. Martell, R. M. Smith, *Critical Stability Constants, Vol. 2*, Plenum, New York, **1974**.
- [24] Gaussian 03, Revision B.05, M. J. Frisch, G. W. Trucks, H. B. Schlegel, G. E. Scuseria, M. A. Robb, J. R. Cheeseman, J. A. Montgomery, Jr., T. Vreven, K. N. Kudin, J. C. Burant, J. M. Millam, S. S. Iyengar, J. Tomasi, V. Barone, B. Mennucci, M. Cossi, G. Scalmani, N. Rega, G. A. Petersson, H. Nakatsuji, M. Hada, M. Ehara, K. Toyota, R. Fukuda, J. Hasegawa, M. Ishida, T. Nakajima, Y. Honda, O. Kitao, H. Nakai, M. Klene, X. Li, J. E. Knox, H. P. Hratchian, J. B. Cross, V. Bakken, C. Adamo, J. Jaramillo, R. Gomperts, R. E. Stratmann, O. Yazyev, A. J. Austin, R. Cammi, C. Pomelli, J. W. Ochterski, P. Y. Ayala, K. Morokuma, G. A. Voth, P. Salvador, J. J. Dannenberg, V. G. Zakrzewski, S. Dapprich, A. D. Daniels, M. C. Strain, O. Farkas, D. K. Malick, A. D. Rabuck, K. Raghavachari, J. B. Foresman, J. V. Ortiz, Q. Cui, A. G. Baboul, S. Clifford, J. Cioslowski, B. B. Stefanov, G. Liu, A. Liashenko, P. Piskorz, I. Komaromi, R. L. Martin, D. J. Fox, T. Keith, M. A. Al-Laham, C. Y. Peng, A. Nanayakkara, M. Challacombe, P. M. W. Gill, B. Johnson, W. Chen, M. W. Wong, C. Gonzalez, J. A. Pople, Gaussian, Inc., Wallingford CT, **2004**.
- [25] a) A. P. de Silva, H. Q. N. Gunaratne, C. P. McCoy, *Chem. Commun.* **1996**, 2399–2400; b) A. Tamayo, C. Lodeiro, L. Escriche, J. Casabó, B. Covelo, P. González, *Inorg. Chem.* **2005**, *44*, 8105–8115.
- [26] a) L. Zhang, R. J. Clark, L. Zhu, *Chem. Eur. J.* **2008**, *14*, 2894–2903; b) A. H. Younes, L. Zhang, R. J. Clark, L. Zhu, *J. Org. Chem.* **2009**, *74*, 8761–8772.
- [27] D. Wang, Y. Shiraishi, T. Hirai, *Chem. Commun.* **2011**, *47*, 2673–2675.
- [28] J. E. Sabol, M. G. Rockley, *J. Photochem. Photobiol. A* **1987**, *40*, 245–257.

Received: April 6, 2011
Published online: June 27, 2011